

ELECTROPRODUCTION OF RHO AND PHI MESONS\*

J. T. Dakin, G. J. Feldman, W. L. Lakin,\*\*  
F. Martin, M. L. Perl, E. W. Petraske,† W. T. Toner††

Stanford Linear Accelerator Center  
Stanford University, Stanford, California 94305

ABSTRACT

We report measurements of  $\rho^0$  and  $\phi$  electroproduction at 19.5 GeV in a wide-aperture spectrometer which detected the scattered electron and the decay products of the vector mesons. As  $|q^2|$  increases, the rho mass spectrum shape changes, the momentum transfer distribution broadens, and the ratio of the rho cross section to the total cross section decreases. The ratio of longitudinally to transversely polarized  $\rho^0$  mesons is  $.45 \begin{smallmatrix} + .15 \\ - .10 \end{smallmatrix}$  at  $|q^2| = m_\rho^2$ , and the interference between longitudinal and transverse amplitudes is almost maximal. The relative  $\phi$  meson cross section also decreases as  $|q^2|$  increases.

(Submitted to Phys. Rev. Letters)

---

\*Work supported by the U. S. Atomic Energy Commission.

\*\*Present address: Birmingham Radiation Centre, University of Birmingham, P. O. Box 363, Birmingham B15 2TT, England.

†Present address: Vanderbilt University, Nashville, Tennessee 37203.

††Present address: Rutherford High Energy Laboratory, Chilton, Didcot, Berkshire, England.

Many photoproduction processes can be understood by assuming that the photon couples directly to vector meson states. By studying vector meson electroproduction we seek to determine how this coupling evolves as the photon becomes space-like and its polarization has longitudinal as well as transverse components. We report here a measurement of rho electroproduction which combines high virtual photon energies and the ability to study rho production and decay angular correlations.<sup>1</sup>

The rho electroproduction reaction

$$ep \rightarrow ep \pi^+ \pi^- \quad (1)$$

can be regarded as an inelastic electron scatter ( $e \rightarrow e\gamma^*$ ) followed by the virtual photoproduction of a rho ( $\gamma^*p \rightarrow \rho p$ ) followed by the rho decay ( $\rho \rightarrow \pi^+ \pi^-$ ). Quantities describing the electron scatter are  $q^2$ , the photon mass squared,  $\epsilon$ , the photon polarization, and  $s$ , the c.m. energy squared in the  $\gamma^*p$  collision. The rho production is characterized by  $t'$ , the four momentum transfer squared to the proton less its smallest possible value ( $t'_{\min}$ ), and  $\phi_e$ , the azimuthal angle between the electron scatter plane and the rho production plane. The final  $\pi^+ \pi^-$  system is described by its invariant mass,  $m_{\pi\pi}$ ,  $\phi$ , the azimuthal angle between the rho production plane and the rho decay plane, and  $\theta$ , the rho decay polar angle. The angle  $\psi \equiv \phi_e + \phi$  is the angle between the electron scatter plane and the rho decay plane in the limit  $t' \rightarrow 0$ . We use the same angle conventions as Dieterle.<sup>2</sup>

The experimental apparatus, which has been described elsewhere,<sup>3</sup> consisted of a 19.5 GeV/c electron beam incident on a hydrogen target followed by a large-aperture magnetic spectrometer. The optical spark chambers were triggered by an array of shower counters each time an incident electron scattered more than 30 mrad from the beam with an energy  $E' \gtrsim 4$  GeV.

All of the film was measured by a flying-spot digitizer and selected samples were also measured by a conventional manual system. Scattered electrons were identified as tracks whose momenta matched the appropriate shower counter pulse heights. All other tracks were assumed to be hadrons. The number of electrons in each  $q^2$ -s interval was corrected for geometric efficiency, measuring losses, hadron contamination (0 to 7%) and radiative effects (10 to 48%).<sup>4</sup> The result was the total number of virtual photon interactions in the data in that  $q^2$ -s interval, or effectively the  $\gamma^*p$  total cross section,  $\sigma_{\text{tot}}(q^2, s)$ .

Each event with 3 or more tracks was measured up to 3 times by the manual system to see whether it contained an  $e, \pi^+, \pi^-$  combination consistent with a 1-c fit to reaction (1). The missing (proton) mass squared interval allowed was from 0.2 to 1.6  $\text{GeV}^2$ . There were 238 "rho" events surviving this process in the kinematic range  $-0.25 > q^2 > -2.00 (\text{GeV}/c)^2$ ,  $10 < s < 30 (\text{GeV})^2$ ,  $0 > t' > -0.7 (\text{GeV}/c)^2$ , and  $0.6 < m_{\pi\pi} < 0.9 \text{ GeV}$ . These events were divided into 3  $q^2$  bins whose average properties were  $q^2$  (-.36, -.70, -1.27),  $s$ (22.6, 19.6, 19.8),  $\epsilon$  (.67, .74, .72) and  $t_{\text{min}}$  (-.008, -.015, -.033).

The events in each bin were fit by a maximum-likelihood technique to the form

$$\frac{d\sigma_{\rho}(q^2, s)}{dt'd\phi_e d\psi d\cos\theta} = \sigma_{\text{tot}}(q^2, s) \frac{\sigma_{\rho}}{\sigma_{\text{tot}}} b e^{bt'} W(\phi_e, \psi, \theta) \quad . \quad (2)$$

The fitting function contained the normalization  $\sigma_{\text{tot}}(q^2, s)$  determined by counting electrons and the detailed dependence of the geometric efficiency on the independent variables  $q^2, s, t, \phi_e, \psi, \cos\theta$ . The output from the fit included the ratio  $\sigma_{\rho}/\sigma_{\text{tot}}$ , the slope parameter  $b$ , and parameters from the angular correlation term,  $W$ , to be described later.

The normalized cross section,  $\sigma_\rho/\sigma_{\text{tot}}$ , was corrected for elastic  $\rho$  losses due to radiation (24%),<sup>5</sup> the missing mass cut (9%), the  $m_{\pi\pi}$  cut (29%), scanning and measuring losses (10%), and numerous small instrumental effects (13%). A correction was also made for the number of  $\pi\pi$  events in the  $m_{\pi\pi}$  interval used which were not elastic  $\rho$  events (5%). The overall systematic uncertainty in  $\sigma_\rho/\sigma_{\text{tot}}$  is estimated to be 16%. The error bars indicated in the figures represent statistical errors only.

Figure 1 shows the invariant mass distribution of all pion pairs consistent with the hypothesis of reaction (1). The dipion mass spectrum is dominated by the  $\rho^0$  meson with little or no background. Some of the events with dipion mass less than .4 GeV are consistent with the hypothesis



These events will be discussed later.

To study possible changes in the  $\rho^0$  mass spectrum as a function of  $q^2$ , we fit the data in the range  $0.44 < m_{\pi\pi} < 1.04$  GeV in each  $q^2$  bin to the form

$$\frac{d\sigma}{dm_{\pi\pi}} = \left( \frac{m_\rho^2}{m_{\pi\pi}^2} \right)^{n/2} B(m_{\pi\pi}) \quad (4)$$

where  $B(m_{\pi\pi})$  is a relativistic p-wave Breit-Wigner shape<sup>6</sup> with the mass (= .77 GeV) and width (= .145 GeV) fixed at photoproduction values.<sup>7</sup> The photoproduction data were fit in an identical manner. All of the data were fit well by Eq. (4). When a flat background term was added to Eq. (4), the fit values of  $n$  did not change appreciably and backgrounds selected by the fits were between 0 and 5%. The fit values of  $n$  are shown in Fig. 2a. The  $\rho$  mass shape appears to become more "normal" as  $|q^2|$  increases. This effect was predicted by a diffraction-dissociation model,<sup>8</sup> but the prescription given by

that model,

$$\left( \frac{m_\rho^2}{m_\pi^2} \right)^{n/2} \rightarrow \left( \frac{m_\rho^2 - q^2}{m_\pi^2 - q^2} \right)^{n/2} \quad (5)$$

provides a more drastic change in the rho mass spectrum for  $|q^2| \lesssim m_\rho^2$  than is indicated by the data.

We fit  $t'$  distributions to the form  $e^{bt'}$  in the range  $0 > t' > -.7$  (GeV/c)<sup>2</sup> in each of the  $q^2$  bins. The results of these fits are shown in Fig. 2b along with photoproduction results,<sup>7,9</sup> which have been analyzed in the same manner as our data. The  $b$  parameter appears to decrease with increasing  $|q^2|$ . We have attempted to determine the  $t'$  distribution separately for longitudinally and transversely polarized  $\rho^0$  mesons and have found no significant difference between them.

The complete angular distributions for the production and decay of vector mesons have been given by Dieterle.<sup>2</sup> We have studied the angular correlations in the data for evidence for nonhelicity-conserving amplitudes and have failed to find any at the 10% level. Thus we have assumed that s-channel helicity conservation holds in electroproduction, as it does in photoproduction, and have fit the data to the angular distribution,

$$W(\theta, \psi) = \frac{3}{8\pi^2(1+\epsilon R)} \left[ \epsilon R \cos^2 \theta + \frac{1}{2} \sin^2 \theta (1+\epsilon \cos 2\psi) - (\epsilon R(1+\epsilon)/2)^{\frac{1}{2}} \cos \delta \sin 2\theta \cos \psi \right], \quad (6)$$

where  $R$  is the production ratio of longitudinally to transversely polarized  $\rho^0$  mesons and  $\delta$  is the phase angle between the longitudinal and transverse amplitudes. The results of the fits for  $R$  and  $\cos \delta$  are given in Figs. 2c and 2d. For a purely diffractive production process  $\cos \delta$  should be unity.

Sakurai and Schildknecht have tried to understand inelastic electron-proton scattering in terms of the production of vector meson states.<sup>10</sup> (We refer to this paper as the VMD model.) We have fit R to the form suggested by this model,

$$R = -\xi^2 \frac{q^2}{m_\rho^2} \quad (7)$$

The data are adequately described by this fit with  $\xi^2 = .45^{+.15}_{-.10}$ ; however this value of  $\xi^2$  does not appear to be consistent with the value required by the VMD model to fit inelastic electron scattering results, ( $\xi^2 \approx .06$ ). The data are somewhat better described by the Ansatz suggested by Eckardt et al.,<sup>11</sup>

$$R = \frac{-q^2}{m_\rho^2 - q^2} \quad (8)$$

Figure 2e shows the ratio of the  $\rho^0$  virtual photoproduction cross section to the total virtual photoproduction cross section. Photoproduction cross section ratios, which were obtained by similar analysis methods, are also shown. The  $\rho^0$  cross section drops faster than the total virtual photoproduction cross section and also faster than the prediction of the VMD model,

$$\left. \frac{d\sigma(q^2)}{dt} \right|_{t=0} = \left. \frac{d\sigma(0)}{dt} \right|_{t=0} \frac{(1 - \epsilon \xi^2 q^2 / m_\rho^2)}{(1 - q^2 / m_\rho^2)^2} \quad (9)$$

We note, however, that the data can be described by the simple form,

$$\sigma_\rho(q^2) = \sigma_\rho(0) \frac{e^{bt_{\min}}}{(1 - q^2 / m_\rho^2)^2} \quad (10)$$

Both Eqs. (9) and (10) are displayed in Fig. 2e in terms of cross section ratios.

There were 6 events which satisfied the hypothesis of exclusive  $\phi$  meson production, reaction (3). We estimate that the background from electron, muon,

and pion pairs was  $1 \pm 1$  events. The average  $q^2$  of the events was  $-.6$  (GeV/c)<sup>2</sup> and the average  $s$  was  $22.9$  GeV<sup>2</sup>. The acceptance for  $\phi$ 's was 60% larger than that for  $\rho^0$ 's; the corrections were similar except for meson mass cut (0%),  $k$  decay (42%), and unseen decay modes (104%). The ratio of the  $\phi$  virtual photoproduction cross section to the total virtual photoproduction cross section is  $.0017 \pm .0009$  compared to  $.0046 \pm .0006$  for photoproduction.<sup>7</sup>

We are indebted to C. A. Lichtenstein and to W. Atwood and S. Stein for supplying us with computer programs for the evaluation of radiative corrections. We are grateful to D. Schildknecht for illuminating discussions on aspects of the VMD model.

#### REFERENCES

1. The current status of experimental results in this field has been summarized by K. Berkelman, Invited talk at the XVI International Conference on High Energy Physics, NAL, Batavia, Illinois, September 1972, Cornell Report No. CLNS-194 (1972), to be published.
2. B. Dieterle, *Nuovo Cimento* 11A, 523 (1972). The angles indicated in Fig. 2 of this reference are positive.
3. J. T. Dakin, G. J. Feldman, W. L. Lakin, F. Martin, M. L. Perl, E. W. Petraske, and W. T. Toner, *Phys. Rev. Letters* 29, 746 (1972) and SLAC Report No. SLAC-PUB-1074 (1972), unpublished.
4. G. Miller, SLAC Report No. SLAC-129 (1971), unpublished.
5. A. Bartl and P. Urban, *Acta Physica Austriaca* 24, 139 (1966).
6. J. D. Jackson, *Nuovo Cimento* 34, 1645 (1964). Equations 4, A.1, and A.2.
7. J. Ballam, G. B. Chadwick, Y. Eisenberg, E. Kogan, K. C. Moffeit, P. Seyboth, I. O. Skillicorn, H. Spitzer, G. Wolf, H. H. Bingham, W. B. Fretter, W. J. Podolsky, M. S. Rabin, A. H. Rosenfeld and

G. Smadja, SLAC Report No. SLAC-PUB-1143 (1972), to be published.

We use the 9.3 GeV data only.

8. M. Ross and L. Stodolsky, Phys. Rev. 149, 1172 (1966).
9. F. Bulos, W. Busza, R. Giese, E. Kluge, R. Larsen, D.W.G.S. Leith, and S. H. Williams, Contribution to the XVI International Conference on High Energy Physics, NAL, Batavia, Illinois, September 1972 (unpublished).

We use 9 to 13 GeV data only.

10. J. J. Sakurai and D. Schildknecht, Phys. Letters 40B, 121 (1972).
11. V. Eckardt, H. J. Gebauer, P. Joos, H. Meyer, B. Naroska, D. Notz, W. J. Podolsky, G. Wolf, S. Yellin, G. Drews, H. Nagel, and E. Rabe, Contribution to the XVI International Conference on High Energy Physics, NAL, Batavia, Illinois, September 1972 (unpublished).

#### FIGURE CAPTIONS

1. Dipion mass spectrum for all events in which the missing mass is consistent with that of a proton. The curve represents the relative acceptance averaged over all other variables.
2. (a) The parameter  $n$  defined in Eq. (4). (b) The  $b$  parameter from fits to the form  $e^{bt}$ . (c) The ratio of longitudinal to transverse  $\rho^0$  production. The dotted line is the best fit to Eq. (7). (d) Cosine of the longitudinal-transverse phase difference. (e) The ratio of the  $\rho^0$  virtual photoproduction cross section to the total virtual photoproduction cross section. The solid curve represents the prediction of the VMD model, Eq. (9), and the dashed curve represents Eq. (10). Photoproduction data ( $q^2=0$ ) are taken from Refs. 7 and 9.

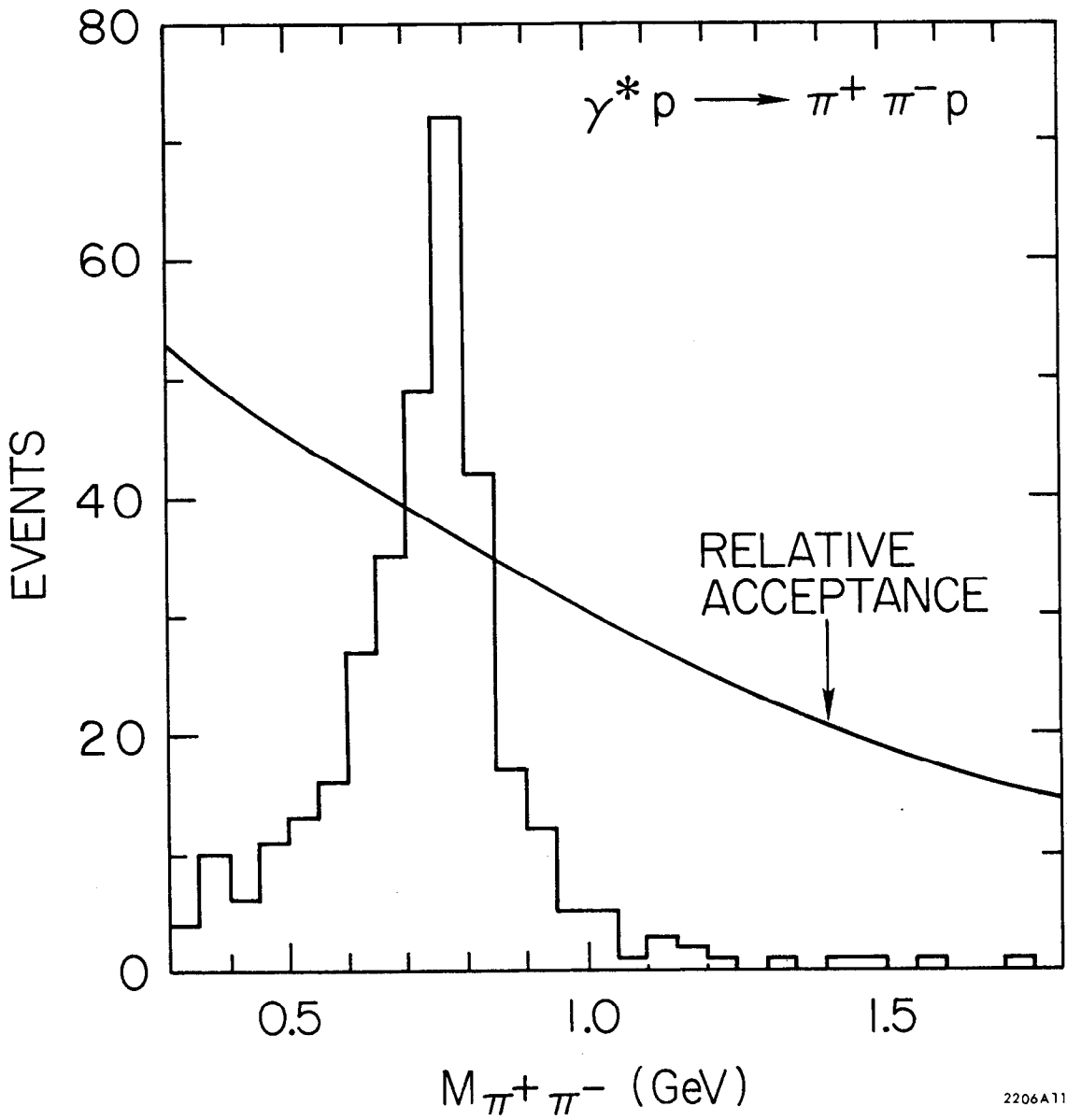
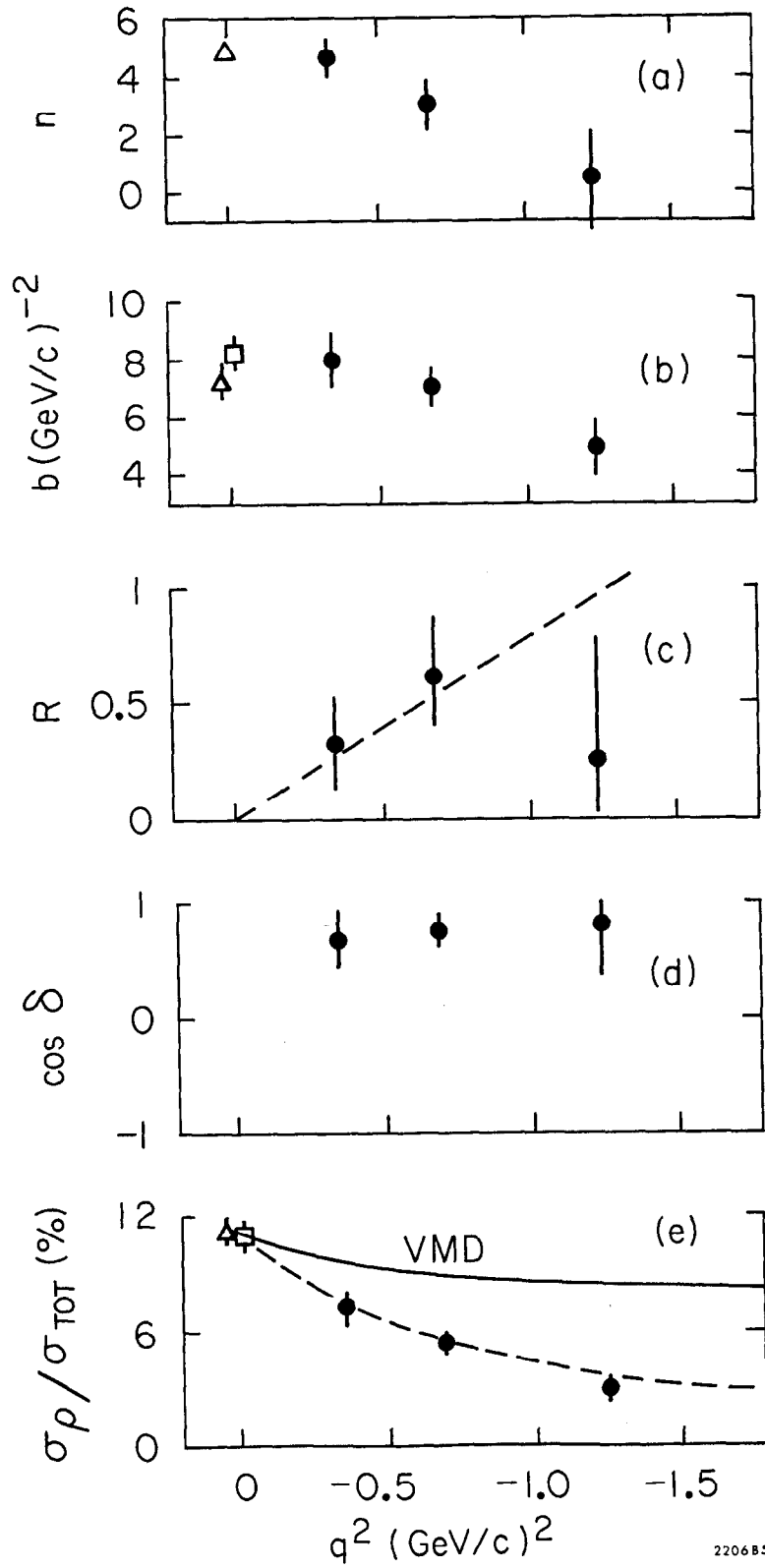


Fig. 1

$\Delta$  Ballam et al.     $\bullet$  This Experiment  
 $\square$  Bulos et al.



220685

Fig. 2